J Toxicol Pathol 2024; 37: 83–91

Original Article

Neural tissue tolerance to synthetic dural mater graft implantation in a rabbit durotomy model

Yuval Ramot[1,2a], Noam Kronfeld[3a], Michal Steiner[4a], Nora Nseir Manassa[5], Amir Bahar[5], and Abraham Nyska[6*]

[1]Department of Dermatology, Hadassah Medical Center, PO Box 12000, Jerusalem, 9112001, Israel
[2]The Faculty of Medicine, Hebrew University of Jerusalem, PO Box 12272, Jerusalem, 9112001, Israel
[3]Envigo CRS (Israel), Einstein St., Building 13B, Weizmann Science Park, Ness Ziona, 7414001, Israel
[4]Pre-Clinical Consultant, Carmel St. 11/22, Rehovot, 7630511, Israel
[5]Nurami Medical Nanofiber Technology, Ha-Namal St 36, Haifa, 303203, Israel
[6]Consultant in Toxicologic Pathology, Tel Aviv and Tel Aviv University, Yehuda HaMaccabi 31, Tel Aviv 6200515, Israel

Abstract: In neurosurgical interventions, effective closure of the dura mater is essential to prevent cerebrospinal fluid leakage and minimize post-operative complications. Biodegradable synthetic materials have the potential to be used as dura mater grafts owing to their regenerative properties and low immunogenicity. This study evaluated the safety of ArtiFascia, a synthetic dura mater graft composed of poly(l-lactic-co-caprolactone acid) and poly(d-lactic-co-caprolactone acid), in a rabbit durotomy model. Previously, ArtiFascia demonstrated positive local tolerance and biodegradability in a 12-month preclinical trial. Here, specialized stains were used to evaluate potential brain damage associated with ArtiFascia use. Histochemical and immunohistochemical assessments included Luxol Fast Blue, cresyl Violet, Masson's Trichrome, neuronal nuclei,, Glial Fibrillary Acidic Protein, and ionized calcium-binding adaptor molecule 1 stains. The stained slides were graded based on the brain-specific reactions. The results showed no damage to the underlying brain tissue for either the ArtiFascia or control implants. Neither inflammation nor neuronal loss was evident, corroborating the safety of the ArtiFascia. This approach, combined with previous histopathological analyses, strengthens the safety profile of ArtiFascia and sets a benchmark for biodegradable material assessment in dura graft applications. This study aligns with the Food and Drug Administration guidelines and offers a comprehensive evaluation of the potential neural tissue effects of synthetic dura mater grafts. (DOI: 10.1293/tox.2023-0121; J Toxicol Pathol 2024; 37: 83–91)

Key words: dura mater, biodegradability, brain, immunohistochemistry, biodegradation

Introduction

The dura mater is the outermost and toughest layer of the meninges and plays a crucial role in safeguarding the brain[1–4]. It provides essential mechanical support to the brain and controls blood drainage from the brain through the dural sinuses. Comprised mainly of collagen fibers, the dura mater further contains dispersed fibroblasts and elastin fibers that are situated within an extracellular matrix[5–8].

Certain neurosurgical procedures, including the surgical extraction of tumors, hematomas, and meningiomas, require dural resection, which could consequently lead to postoperative cerebrospinal fluid (CSF) leakage. This is recognized as a significant complication that can result in substantial health challenges. CSF leakage occurs in up to 13% of elective neurosurgical procedures[9]. Hence, ensuring effective closure of the dura mater is of paramount significance in neurosurgical interventions[9]. Beyond preventing CSF leakage, proper closure also diminishes the risk of postoperative infections, arachnoiditis, and neural damage[10].

Occasionally, the use of a dural graft is necessary to seal the residual post-operative dural defects. These grafts, known as autologous grafts, can be sourced from the patient's tissues, such as the fascia lata, temporal fascia, and galea aponeurotica. These grafts are not only cost-effective but also exhibit favorable biological qualities. Nevertheless, not all patients have adequate tissue available for grafting, and acquiring an autologous graft involves a time-intensive process, which adds complexity to the surgery and increases the potential for infection[11–14]. Various xenografts have also been proposed, such as the bovine pericardium and collagen

Received: 14 November 2023, Accepted: 9 January 2024
Published online in J-STAGE: 12 February 2024
[a]These authors contributed equally.
*Corresponding author: A Nyska (e-mail: anyska@nyska.net)
(Supplementary material: refer to PMC https://www.ncbi.nlm.nih.gov/pmc/journals/1592/)

matrix. However, these alternatives can lead to several undesirable outcomes, including graft dissolution, body rejection, inflammatory reactions, scarring, and adhesions[10, 15].

Biodegradable synthetic materials exhibit numerous essential properties and can serve as dural grafts. They promote tissue regeneration and gradually dissolve as native neodura forms without triggering immune or inflammatory responses. These materials are convenient to manipulate and suture, in addition to being cost-effective[16–19]. Numerous such materials have been assessed as potential dura mater grafts[3, 17, 20–23]. However, their utilization remains constrained, as very few products are commercially available, and these synthetic materials, especially non-degradable ones, may give rise to instances of inflammatory granulomatous foreign body reactions, which can have severe consequences in certain cases[10, 24]. Moreover, the effects of these materials on neural tissues remain a subject of ongoing investigation. Consequently, a comprehensive preclinical evaluation of new biodegradable materials for dural graft applications is imperative. This can be achieved by employing suitable animal models and conducting thorough histopathological assessments of the implanted tissues.

ArtiFascia (Nurami Medical Nanofiber Technology, Haifa, Israel) is an innovative synthetic fibrous scaffold featuring a porous structure crafted from poly(l-lactic-co-caprolactone acid) (PLCL) and poly(d,l-lactic-co-caprolactone acid) (PDLCL). It has been specifically developed as a dura mater graft, and its constituents have not been used previously for this clinical indication. Notably, it was recently approved by the Food and Drug Administration (FDA) for the treatment of cranial dural defects. In an earlier study, we examined the biodegradability and local compatibility of ArtiFascia in a 12-month preclinical trial involving rabbits. This evaluation was performed in comparison with a bovine collagen matrix, which served as a reference control. Our findings revealed that ArtiFascia exhibits notably positive local tolerance and a promising biodegradability profile. This was evident through the formation of new dura mater tissue at the implantation site, along with the restoration of dural integrity and the overlying calvaria bone[19]. Nonetheless, the possibility of neural damage in the underlying neural tissue should be investigated due to the persistence of ongoing mild inflammation inherent in the typical foreign body response. This includes the possibility of issues such as compressive injury or inflammation.

In this study, our objective was to delve deeper into the possibility of brain damage stemming from ArtiFascia use. To achieve this, we employed specialized stains designed to label distinct constituents of brain tissue. These stains play a crucial role in enhancing our understanding of the ongoing inflammatory responses associated with ArtiFascia devices. Moreover, they aid in excluding the presence of inflammation and neuronal degeneration, such as astrocytosis and/or microgliosis in the underlying cortex. As in our previous study, a collagen dural graft was used as a reference control.

Materials and Methods

Test and reference control items

The test material under examination was ArtiFascia, a new synthetic fibrous scaffold crafted for dura mater grafting, featuring a distinctive porous structure. ArtiFascia is constructed from a matrix of PLCL and PDLCL. The dural repair matrix used for comparison was Duragen® (Integra LifeSciences Corp., Plainsboro, NJ, USA), a commercially accessible product manufactured from processed bovine collagen, derived from the deep flexor tendon of bovines. This matrix had a porous spongy structure.

Animal model and experimental design

For the special stain assessments, we utilized slides collected from animals previously euthanized as part of the earlier local tolerability and biodegradability pre-clinical study[19]. In brief, a total of eighteen HsdOkd: NZW male rabbits, aged approximately 3–5 months, were sourced from Envigo RMS (Jerusalem, Israel). All animals underwent dural defect induction and subsequent implantation (Table 1). Details of dural defect induction are provided by Ramot *et al.*[19], in brief, we drilled 8 mm holes on both sides of the parietal bone, going through the calvarial bone using a trephine burr, while keeping the area irrigated with saline. The holes reached the level of the dura. For accurate repositioning of the bone piece to its original alignment, a small hole (approximately 2.0 mm in diameter) was drilled through the outer surface of the bone nearest the nose (referred to as '12 o'clock'). Using a biopsy punch and scissors, a round piece measuring 4 mm in diameter was removed from the underlying dura mater of each of the created bone defects. Each dural defect was fully covered using a 6 mm segment of either ArtiFascia or the Reference control material, placed without suturing. Animals were euthanized at 1, 6, and 12 months post-implantation (2, 3, and 4 animals per test or reference control item and per respective termination period, as indicated in Table 1). The study was conducted following the receipt of authorization from the National Council for Animal Experimentation (No. IL-16-03-72).

After the experimental period, the animals were euthanized and subjected to perfusion, and the skull and brain were sectioned along the coronal plane on both sides of the defects, while the implanted devices remained in place. This was achieved using an Exakt diamond bandsaw. Subsequently, the samples were prepared without the use of

Table 1. Experimental Design

Group	Group size (No. of animals)	Implanted device	*Observation period* (Months post-surgery)
1	2	*Reference Control*	1
	3		6
	4		12
2	2	*ArtiFascia®*	1
	3		6
	4		12

xylene, processed, embedded in paraffin, and then sliced into sections with an approximate thickness of 5 µm. All sections were stained with Hematoxylin and Eosin (H&E). For histochemical and immunohistochemical staining, sections were selected from 2 animals at the 1-month termination point, 3 animals at the 6-month termination point, and 3 animals at the 12-month termination point. These sections were obtained from both the ArtiFascia and the reference control groups. The slides were stained (one stain per slide) with Luxol Fast Blue (LFB; including cresyl Violet counterstain per standard staining convention), cresyl Violet, and Masson's trichrome (MT). Immunohistochemistry was performed using the following antibodies, neuronal nuclei (NeuN) Immunohistochemistry (IHC), Glial Fibrillary Acidic Protein (GFAP), and ionized calcium-binding adaptor molecule 1 (Iba-1) (Table 2).

We used a modified grading system to evaluate brain immunostaining, using a scale of 0–4[25, 26]:

• Grade 0: When there was no noticeable positive staining in the included brain sections, we marked them as "–."
• Grade 1: We used "+/–" when staining was observed in the included brain sections, but was either focal, along the periphery, or only in a small number of cells.
• Grade 2: "+" indicates positive staining in a significant portion of cells within the included brain section, usually with a more widespread distribution across the lesion.
• Grade 3: A higher grade (++) was assigned for positive staining observed in an increasing number of cells within the included brain sections.
• Grade 4: An even higher grade (+++) was assigned when positive staining was observed in a growing number of cells within the included brain sections.

Results

Survival

No animal experienced any treatment-related deaths or unusual clinical signs during the 12-month observation period.

Hematoxylin and Eosin stain

The H&E staining results for both the reference control and ArtiFascia-implanted slides were detailed in a prior report[19]. Briefly, the staining illustrated the gradual degradation of the implanted graft, which was completely absorbed by the end of the 12 months. Neodura formation was evident along with the recovery of both the dural damage and the calvarial bone above it. The ArtiFascia device prompted a foreign body reaction marked by the presence of macrophages and giant cells encompassed by a fibrotic capsule. No other inflammatory reactions were observed within the cavities, capsules, or the surrounding brain tissue. Figure 1A, 1B, and the inset depict representative H&E-stained slides. The reference control device was completely degraded by the 6-month termination time point, leaving an empty cavity surrounded by a thin capsule. No inflammatory reactions were observed within the capsule or adjacent brain tissue. The implantation site was completely covered with the newly formed mature bone. There was also evidence of neodura formation at the surgical site, suggesting progressive healing of the previously induced dural defect.

Cresyl violet staining

Cresyl violet staining is not specifically targeted at neurons; rather, its appearance is a result of the abundant concentration of "Nissl substance" found in neurons[27–29]. Nevertheless, this staining method is still commonly employed for neuronal tissue because of its affinity for the acidic components of the neuronal cytoplasm, including ribosomes rich in RNA, as well as the nucleoli of the cells[27, 29]. Cresyl violet staining of the implanted sites did not reveal any irregularities within the adjacent brain tissues in either the reference control or ArtiFascia-treated animals (Fig. 1C and 1D, Supplementary Table 1).

Glial fibrillary acidic protein staining

GFAP is a subunit of the intermediate filaments present in glial cells[30]. These characteristics have been exploited in biochemical, immunological, and biological studies. Furthermore, GFAP reliably serves as a marker for benign astrocytes and neoplastic cells of glial origin. GFAP staining of the implantation sites in animals treated with both the reference control and ArtiFascia did not reveal any anomalies (Fig. 1E and 1F, Supplementary Table 1).

Ionized calcium-binding adaptor molecule-1 staining

Iba-1 is a calcium-binding protein predominantly found in microglia in the brain[31–35]. This distinct localization of Iba-1 suggests that it is significantly involved in the regulation of microglial function. Iba-1 staining performed on the implantation sites of animals subjected to both the reference control and ArtiFascia treatments did not reveal any irregularities (Fig. 2A and 2B, Supplementary Table 1).

Table 2. Immunohistochemistry Details

Target marker	Primary antibody description	Vendor (Catalog)	Clone	Dilution factor	Secondary (Vendor)	Detection kit
NeuN	Monoclonal mouse anti-NeuN	Bio SB (BSB 2007)	A60	1:250	Mouse-on-Canine HRP-Polymer (Biocare)	SignalStain® DAB Substrate Kit
GFAP	Monoclonal mouse anti-GFAP	Bio SB (BSB 5566)	G-A-5	1:500	Mouse-on-Canine HRP-Polymer (Biocare)	SignalStain® DAB Substrate Kit
Iba-1	Polyclonal rabbit biotin-conjugated anti-IBA1	FUJIFILM Wako (016-26461)	Not Available	1:100	4 Plus Streptavidin-HRP (Biocare)	SignalStain® DAB Substrate Kit

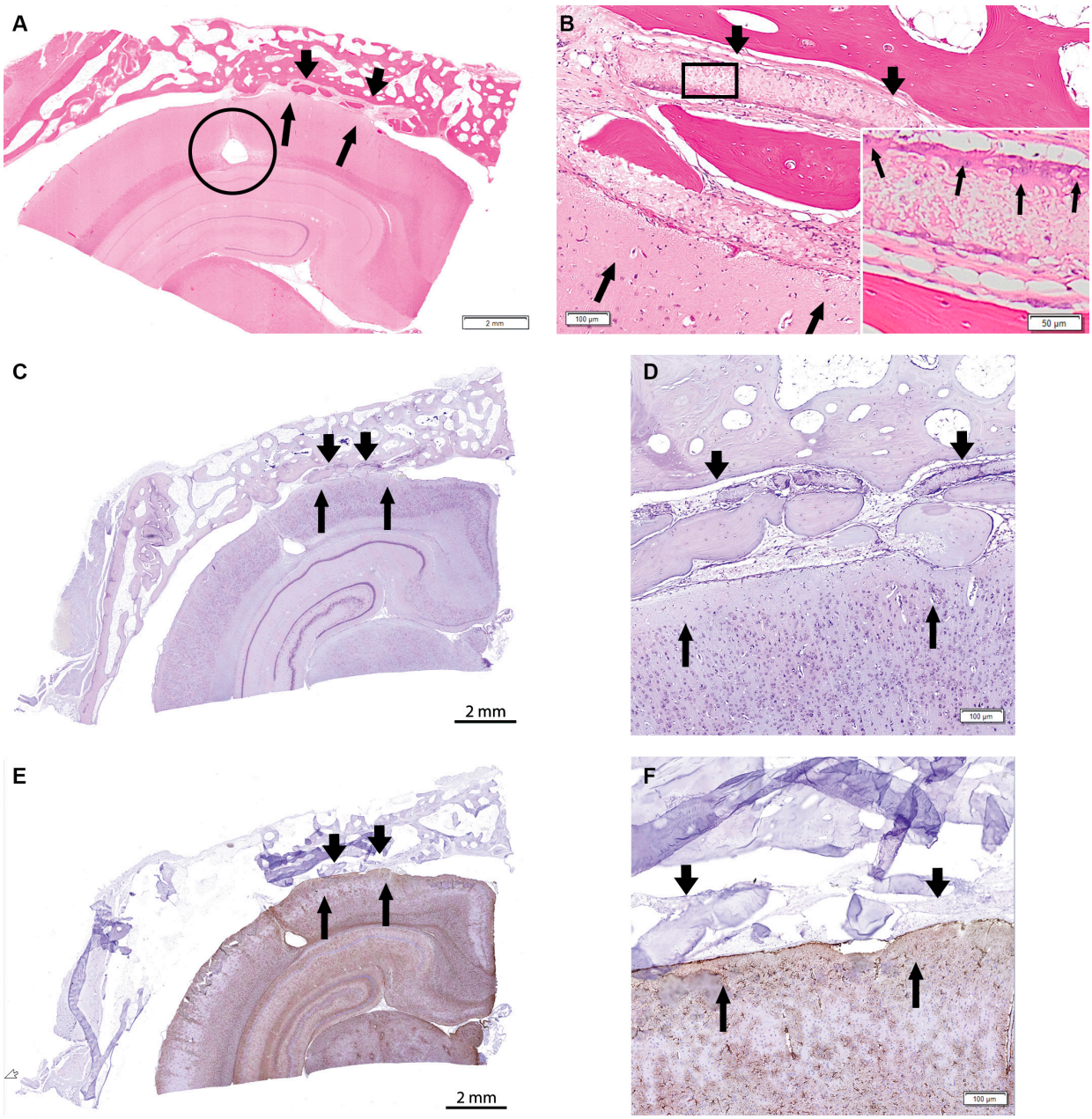

Fig. 1. **A and B.** Hematoxylin and Eosin staining taken from the right implantation site of an animal with ArtiFascia after 12 months (A, low magnification; B, high magnification). The implanted device is apparent within the dura mater, comprising two layers of cavities filled with macrophages and giant cells (indicated by thick arrows), all enclosed by a delicate mature fibrotic capsule. Notably, trabecular bone formation is present, indicating progressing maturation over time. Each layer of the test device shows a considerable presence of macrophages and multinucleated giant cells (mild grade), with the absence of a dense network of interwoven clear fibers that typically reflect the polymer nature of the device. This observation suggests the complete absorption of the polymeric component of the device. Sparse ghost remnants of the implanted mesh may be observed (marked by the empty rectangle), but due to their minimal presence, the absorption is deemed complete. No additional inflammatory reaction is evident within the cavities, capsule, or in the surrounding brain tissue (as shown by thin arrows), highlighting its good tolerability. The implantation site is fully enveloped by newly formed mature bone. There's also evidence of neo-dura formation at the operation site, signifying the complete healing of the previously induced dural defect. Additionally, a circle marks the presence of a cyst, considered to be an incidental finding[49]. Inset: The implant at a higher magnification. Arrows point to macrophages and giant cells. **C and D.** Cresyl violet staining of the right implantation site of an animal implanted with ArtiFascia after 12 months (C, low-magnification; D, high-magnification). Thin arrows indicate the brain and thick arrows indicate the skull at the implantation site. Brain; no abnormalities detected. **E and F.** Glial fibrillary acidic protein staining obtained from the right implantation site of an animal implanted with ArtiFascia after 12 months (E, low magnification; F, high magnification). Thin arrows denote the brain, while thick arrows signify the skull at the implantation site. Brain; no abnormality detected.

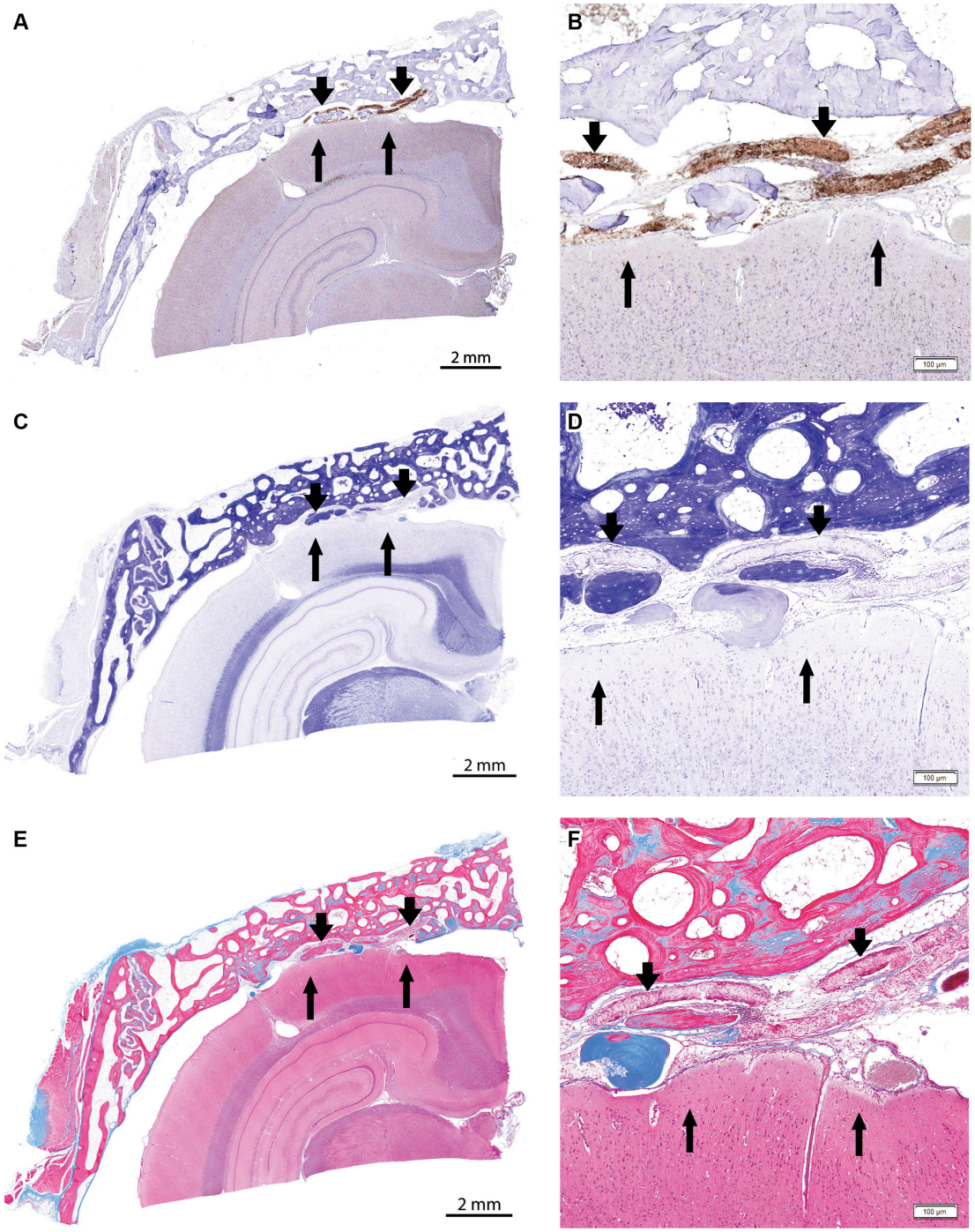

Fig. 2. **A and B.** Ionized calcium-binding adaptor molecule 1 staining acquired from the right implantation site of an animal implanted with ArtiFascia after 12 months (A, low magnification; B, high magnification). Thin arrows denote the brain, while thick arrows represent the skull at the implantation site. Brain; no abnormality detected. **C and D.** Luxol fast blue staining of the right implantation site of an animal implanted with ArtiFascia after 12 months (C, low-magnification; D, high-magnification). Thin arrows indicate the brain and thick arrows indicate the skull at the implantation site. Brain; no abnormalities detected. **E and F.** Masson's trichrome staining taken from the right implantation site of an animal with ArtiFascia after 12 months (E, low magnification; F, high magnification). Thin arrows denote the brain, while thick arrows represent the skull at the implantation site. Brain; no abnormality detected.

Luxol fast blue staining

LFB was first introduced by Kluever and Barrera in 1953[36]. This dye contains a copper phthalocyanine chromogen that is insoluble in water yet soluble in alcohol. Its remarkable properties lie in its strong affinity for staining myelin sheaths[36–38]. LFB staining of the implantation sites of animals undergoing both the reference control and ArtiFascia treatments showed no irregularities (Fig. 2C and 2D. Supplementary Table 1).

Masson's trichrome staining

MT staining effectively distinguished the crucial morphological features pertinent to wound healing. These included keratin, hemoglobin, muscle fibers (appearing in red), cytoplasm and adipose cells (displayed as light red or pink), cell nuclei (appearing dark brown to black), and collagen fibers (stained blue)[39]. Employing this staining technique, we assessed the wound-healing process of the dura and discovered no abnormalities in either the reference control or ArtiFascia treatment. No irregularities were observed (Fig. 2E and 2F, Supplementary Table 1).

Neuronal nuclei staining

NeuN is widely expressed in the nuclei of fully developed neurons in various vertebrate nervous system regions. Its presence is consistent among species and remains stable during specific developmental stages. Consequently, NeuN has been regarded as a reliable marker of mature neurons over the last three decades[40–42]. NeuN staining conducted on the implantation sites of animals subjected to both the reference control and ArtiFascia treatments revealed no irregularities (Fig. 3, Supplementary Table 1).

Discussion

ArtiFascia is a new dura mater graft composed of PLCL and PDLCL. This novel graft previously demonstrated excellent safety and tolerability in a 12-month rabbit durotomy model[19]. Implantation showed a gradual degradation process coupled with an expected inflammatory response attributed to the foreign body reaction, demonstrating a longer-term degradation profile in comparison with the reference device, which was attributed to the different constituents of each device. Nonetheless, persistent inflammation at the dural repair site has the potential to harm the underlying brain or spinal cord, including the risk of compressive injury or inflammation. To address these concerns, we comprehensively assessed the underlying brain tissue. Specialized staining was employed to better understand the impact on various components of the brain tissue, including astrocyte staining (GFAP), microglial staining (Iba-1), and myelin staining (LFB). Additionally, two distinct neuronal stains (NeuN and cresyl violet) were incorporated.

The rabbit model has been previously utilized to assess the performance of the fully-synthetic nanofabricated dura substitute compared to a commercially available xenogenic dura substitute, which is considered a clinically relevant animal model[43]. Other studies have also employed rabbits to study the safety and effectiveness of various compounds in dural regeneration and brain damage[44]. In our investigation, we employed a range of histochemical and immunohistochemical staining techniques to investigate glial cell lineage, following recommendations outlined in ISO 10993-6: 2016 for tests after implantation[45], and as discussed by Bradley *et al*[46].

Assessment of the stained slides revealed no discernible impact of the implanted device (ArtiFascia or the reference control) or concurrent inflammatory reaction on the

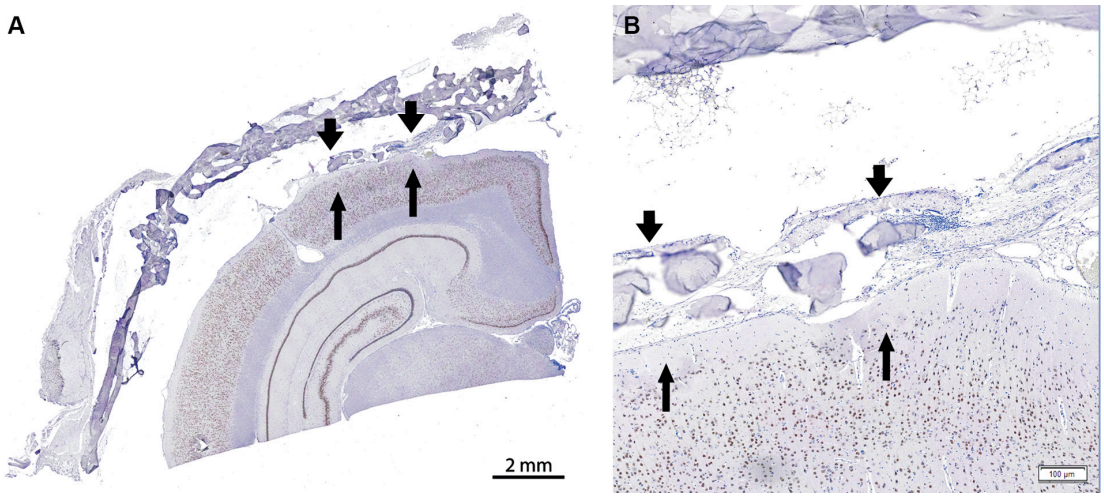

Fig. 3. A and B. Neuronal nuclei staining obtained from the right implantation site of an animal with ArtiFascia after 12 months (A, low magnification; B, high magnification). Thin arrows indicate the brain, while thick arrows denote the skull at the implantation site. Brain; no abnormality detected.

underlying brain tissue. Notably, there was no indication of inflammation in the underlying cortex nor any neuronal loss. These findings, combined with the comprehensive scrutiny of the H&E-stained slides, provide additional robust evidence that reinforces the safety of the implanted material for potential human use.

The recent issuance of the "General Considerations for Animal Studies Intended to Evaluate Medical Devices: Guidance for Industry and Food and Drug Administration Staff" by the US FDA underscores the critical role of properly interpreting tissue responses to a medical device in the FDA's safety evaluation process[47]. The guidance document further underscores the significance of conducting specific assessments such as evaluating inflammation, vascularization, calcification, proteoglycan/collagen, and fibrin/thrombus. Notably, the Medical Device Implant Site Evaluation Working Group of the Society of Toxicologic Pathology Scientific and Regulatory Policy Committee acknowledges that specialized pathology approaches may be necessary to obtain meaningful macroscopic and microscopic data regarding local effects. This report also highlights immunohistochemistry as a valuable method for such assessments[48]. In this study, we adopted this approach by incorporating additional staining methods. This was performed to ensure a comprehensive assessment of the impact of dura mater graft implantation on the brain.

Using these specialized staining techniques, we showed that ArtiFascia did not induce any undesirable effects on the brain. Moreover, the presence of degrading materials and related inflammation did not result in adverse outcomes. We believe that this evaluation approach for dura mater grafts or other devices employed in close proximity to the brain can set a noteworthy standard for future studies that focus on the assessment of biodegradable materials.

Funding Disclosure: The study was funded by Nurami Medical Nanofiber Technology.

Disclosure of Potential Conflicts of Interests: The authors declare the following potential conflicts of interest with respect to the research, authorship, and/or publication of this article: Nora Nseir Manassa and Amir Bahar are employees of Nurami Medical Nanofiber Technology.

References

1. Chuan D, Wang Y, Fan R, Zhou L, Chen H, Xu J, and Guo G. Fabrication and properties of a biomimetic dura matter substitute based on stereocomplex poly(lactic acid) nanofibers. Int J Nanomedicine. **15**: 3729–3740. 2020. [Medline] [CrossRef]
2. Hu Y, Dan W, Xiong S, Kang Y, Dhinakar A, Wu J, and Gu Z. Development of collagen/polydopamine complexed matrix as mechanically enhanced and highly biocompatible semi-natural tissue engineering scaffold. Acta Biomater. **47**: 135–148. 2017. [Medline] [CrossRef]
3. Xie J, Macewan MR, Ray WZ, Liu W, Siewe DY, and Xia Y. Radially aligned, electrospun nanofibers as dural substitutes for wound closure and tissue regeneration applications. ACS Nano. **4**: 5027–5036. 2010. [Medline] [CrossRef]
4. Xu Y, Cui W, Zhang Y, Zhou P, Gu Y, Shen X, Li B, and Chen L. Hierarchical micro/nanofibrous bioscaffolds for structural tissue regeneration. Adv Healthc Mater. **6**: 1601457. 2017. [Medline] [CrossRef]
5. Çavdar S, Sürücü S, Özkan M, Köse B, Malik AN, Aydoğmuş E, Tanış Ö, and Lazoğlu İ. Comparison of the morphologic and mechanical features of human cranial dura and other graft materials used for duraplasty. World Neurosurg. **159**: e199–e207. 2022. [Medline] [CrossRef]
6. Chauvet D, Carpentier A, Allain JM, Polivka M, Crépin J, and George B. Histological and biomechanical study of dura mater applied to the technique of dura splitting decompression in Chiari type I malformation. Neurosurg Rev. **33**: 287–294, discussion 295. 2010. [Medline] [CrossRef]
7. van Noort R, Black MM, Martin TR, and Meanley S. A study of the uniaxial mechanical properties of human dura mater preserved in glycerol. Biomaterials. **2**: 41–45. 1981. [Medline] [CrossRef]
8. Wilcox RK, Bilston LE, Barton DC, and Hall RM. Mathematical model for the viscoelastic properties of dura mater. J Orthop Sci. **8**: 432–434. 2003. [Medline] [CrossRef]
9. Esposito F, Angileri FF, Kruse P, Cavallo LM, Solari D, Esposito V, Tomasello F, and Cappabianca P. Fibrin sealants in dura sealing: a systematic literature review. PLoS One. **11**: e0151533. 2016. [Medline] [CrossRef]
10. Khan Z, Pervez S, and Sharafat S. Comparative analysis of dural substitute autologous vs. semisynthetic collagen-based dura graft. Eur Rev Med Pharmacol Sci. **27**: 3887–3891. 2023. [Medline]
11. Malliti M, Page P, Gury C, Chomette E, Nataf F, and Roux FX. Comparison of deep wound infection rates using a synthetic dural substitute (neuro-patch) or pericranium graft for dural closure: a clinical review of 1 year. Neurosurgery. **54**: 599–603, discussion 603–604. 2004. [Medline] [CrossRef]
12. Mikami T, Minamida Y, Sugino T, Koyanagi I, Yotsuyanagi T, and Houkin K. Free flap transfer for the treatment of intractable postcraniotomy subdural empyemas and epidural abscesses. Neurosurgery. **60**(Suppl 1): ONS83–ONS87, discussion ONS87–ONS88. 2007. [Medline]
13. Nakagawa S, Hayashi T, Anegawa S, Nakashima S, Shimokawa S, and Furukawa Y. Postoperative infection after duraplasty with expanded polytetrafluoroethylene sheet. Neurol Med Chir (Tokyo). **43**: 120–124, discussion 124. 2003. [Medline] [CrossRef]
14. Sun H, Wang H, Diao Y, Tu Y, Li X, Zhao W, Ren J, and Zhang S. Large retrospective study of artificial dura substitute in patients with traumatic brain injury undergo decompressive craniectomy. Brain Behav. **8**: e00907. 2018. [Medline] [CrossRef]
15. Fiorindi A, Gioffrè G, Boaro A, Billeci D, Frascaroli D, Sonego M, and Longatti P. Banked fascia lata in sellar dura reconstruction after endoscopic transsphenoidal skull base surgery. J Neurol Surg B Skull Base. **76**: 303–309. 2015. [Medline] [CrossRef]
16. Pogorielov M, Kravtsova A, Reilly GC, Deineka V, Tetteh G, Kalinkevich O, Pogorielova O, Moskalenko R, and Tkach G. Experimental evaluation of new chitin-chitosan

graft for duraplasty. J Mater Sci Mater Med. **28**: 34. 2017. [Medline] [CrossRef]
17. Wang YF, Guo HF, and Ying DJ. Multilayer scaffold of electrospun PLA-PCL-collagen nanofibers as a dural substitute. J Biomed Mater Res B Appl Biomater. **101**: 1359–1366. 2013. [Medline] [CrossRef]
18. Grotenhuis JA. Costs of postoperative cerebrospinal fluid leakage: 1-year, retrospective analysis of 412 consecutive nontrauma cases. Surg Neurol. **64**: 490–493, discussion 493–494. 2005. [Medline] [CrossRef]
19. Ramot Y, Harnof S, Klein I, Amouyal N, Steiner M, Manassa NN, Bahar A, Rousselle S, and Nyska A. Local Tolerance and biodegradability of a novel artificial dura mater graft following implantation onto a dural defect in rabbits. Toxicol Pathol. **48**: 738–746. 2020. [Medline] [CrossRef]
20. Yamada K, Miyamoto S, Nagata I, Kikuchi H, Ikada Y, Iwata H, and Yamamoto K. Development of a dural substitute from synthetic bioabsorbable polymers. J Neurosurg. **86**: 1012–1017. 1997. [Medline] [CrossRef]
21. Yamada K, Miyamoto S, Takayama M, Nagata I, Hashimoto N, Ikada Y, and Kikuchi H. Clinical application of a new bioabsorbable artificial dura mater. J Neurosurg. **96**: 731–735. 2002. [Medline] [CrossRef]
22. Lavik E, Teng YD, Snyder E, and Langer R. Seeding neural stem cells on scaffolds of PGA, PLA, and their copolymers. Methods Mol Biol. **198**: 89–97. 2002. [Medline]
23. Bernd HE, Kunze C, Freier T, Sternberg K, Kramer S, Behrend D, Prall F, Donat M, and Kramp B. Poly(3-hydroxybutyrate) (PHB) patches for covering anterior skull base defects—an animal study with minipigs. Acta Otolaryngol. **129**: 1010–1017. 2009. [Medline] [CrossRef]
24. Akhaddar A, Turgut AT, and Turgut M. Foreign body granuloma after cranial surgery: a systematic review of reported cases. World Neurosurg. **120**: 457–475. 2018. [Medline] [CrossRef]
25. Fedchenko N, and Reifenrath J. Different approaches for interpretation and reporting of immunohistochemistry analysis results in the bone tissue—a review. Diagn Pathol. **9**: 221. 2014. [Medline] [CrossRef]
26. Fix AS, Ross JF, Stitzel SR, and Switzer RC. Integrated evaluation of central nervous system lesions: stains for neurons, astrocytes, and microglia reveal the spatial and temporal features of MK-801-induced neuronal necrosis in the rat cerebral cortex. Toxicol Pathol. **24**: 291–304. 1996. [Medline] [CrossRef]
27. Alvarez-Buylla A, Ling CY, and Kirn JR. Cresyl violet: a red fluorescent Nissl stain. J Neurosci Methods. **33**: 129–133. 1990. [Medline] [CrossRef]
28. Bartus RT, Dean RL, Cavanaugh K, Eveleth D, Carriero DL, and Lynch G. Time-related neuronal changes following middle cerebral artery occlusion: implications for therapeutic intervention and the role of calpain. J Cereb Blood Flow Metab. **15**: 969–979. 1995. [Medline] [CrossRef]
29. Türeyen K, Vemuganti R, Sailor KA, and Dempsey RJ. Infarct volume quantification in mouse focal cerebral ischemia: a comparison of triphenyltetrazolium chloride and cresyl violet staining techniques. J Neurosci Methods. **139**: 203–207. 2004. [Medline] [CrossRef]
30. McLendon RE, and Bigner DD. Immunohistochemistry of the glial fibrillary acidic protein: basic and applied considerations. Brain Pathol. **4**: 221–228. 1994. [Medline] [CrossRef]
31. Hirasawa T, Ohsawa K, Imai Y, Ondo Y, Akazawa C, Uchino S, and Kohsaka S. Visualization of microglia in living tissues using Iba1-EGFP transgenic mice. J Neurosci Res. **81**: 357–362. 2005. [Medline] [CrossRef]
32. Hwang IK, Yoo KY, Kim DW, Choi SY, Kang TC, Kim YS, and Won MH. Ionized calcium-binding adapter molecule 1 immunoreactive cells change in the gerbil hippocampal CA1 region after ischemia/reperfusion. Neurochem Res. **31**: 957–965. 2006. [Medline] [CrossRef]
33. Imai Y, Ibata I, Ito D, Ohsawa K, and Kohsaka S. A novel gene iba1 in the major histocompatibility complex class III region encoding an EF hand protein expressed in a monocytic lineage. Biochem Biophys Res Commun. **224**: 855–862. 1996. [Medline] [CrossRef]
34. Ito D, Imai Y, Ohsawa K, Nakajima K, Fukuuchi Y, and Kohsaka S. Microglia-specific localisation of a novel calcium binding protein, Iba1. Brain Res Mol Brain Res. **57**: 1–9. 1998. [Medline] [CrossRef]
35. Ito D, Tanaka K, Suzuki S, Dembo T, and Fukuuchi Y. Enhanced expression of Iba1, ionized calcium-binding adapter molecule 1, after transient focal cerebral ischemia in rat brain. Stroke. **32**: 1208–1215. 2001. [Medline] [CrossRef]
36. Kluver H, and Barrera E. A method for the combined staining of cells and fibers in the nervous system. J Neuropathol Exp Neurol. **12**: 400–403. 1953. [Medline] [CrossRef]
37. Carriel V, Garzón I, Alaminos M, and Campos A. Evaluation of myelin sheath and collagen reorganization pattern in a model of peripheral nerve regeneration using an integrated histochemical approach. Histochem Cell Biol. **136**: 709–717. 2011. [Medline] [CrossRef]
38. García-García OD, Weiss T, Chato-Astrain J, Raimondo S, and Carriel V. Staining methods for normal and regenerative myelin in the nervous system. Methods Mol Biol. **2566**: 187–203. 2023. [Medline] [CrossRef]
39. Suvik A, and Effendy AWM. The use of modified Masson's trichrome staining in collagen evaluation in wound healing study. Malays J Vet Res. **3**: 39–47. 2012.
40. Duan W, Zhang YP, Hou Z, Huang C, Zhu H, Zhang CQ, and Yin Q. Novel insights into NeuN: from neuronal marker to splicing regulator. Mol Neurobiol. **53**: 1637–1647. 2016. [Medline] [CrossRef]
41. Huttner HB, Bergmann O, Salehpour M, Rácz A, Tatarishvili J, Lindgren E, Csonka T, Csiba L, Hortobágyi T, Méhes G, Englund E, Solnestam BW, Zdunek S, Scharenberg C, Ström L, Ståhl P, Sigurgeirsson B, Dahl A, Schwab S, Possnert G, Bernard S, Kokaia Z, Lindvall O, Lundeberg J, and Frisén J. The age and genomic integrity of neurons after cortical stroke in humans. Nat Neurosci. **17**: 801–803. 2014. [Medline] [CrossRef]
42. Maxeiner S, Glassmann A, Kao HT, and Schilling K. The molecular basis of the specificity and cross-reactivity of the NeuN epitope of the neuron-specific splicing regulator, Rbfox3. Histochem Cell Biol. **141**: 43–55. 2014. [Medline] [CrossRef]
43. MacEwan MR, MacEwan S, Wright AP, Kovacs TR, Batts J, and Zhang L. Efficacy of a nanofabricated electrospun wound matrix in treating full-thickness cutaneous wounds in a porcine model. Wounds. **30**: E21–E24. 2018. [Medline]
44. Ito K, Horiuchi T, Oyanagi K, Nomiyama T, and Hongo K. Comparative study of fibrin and chemical synthetic sealant on dural regeneration and brain damage. J Neurosurg Spine. **19**: 736–743. 2013. [Medline] [CrossRef]

45. International Organization for Standardization. Biological Evaluation of Medical Devices-Part 6: Tests for Local Effects after Implantation. ISO Standard No. ISO 10993-6. 2016.
46. Bradley AE, Bolon B, Butt MT, Cramer SD, Czasch S, Garman RH, George C, Gröters S, Kaufmann W, Kovi RC, Krinke G, Little PB, Narama I, Rao DB, Sharma AK, Shibutani M, and Sills R. Proliferative and nonproliferative lesions of the rat and mouse central and peripheral nervous systems: new and revised INHAND terms. Toxicol Pathol. **48**: 827–844. 2020. [Medline] [CrossRef]
47. US FDA, General Considerations for Animal Studies Intended to Evaluate Medical Devices: Guidance for Industry and Food and Drug Administration staff, 2023.
48. O'Brien MT, Schuh JCL, Wancket LM, Cramer SD, Funk KA, Jackson ND, Kannan K, Keane K, Nyska A, Rousselle SD, Schucker A, Thomas VS, and Tunev S. Scientific and regulatory policy committee points to consider for medical device implant site evaluation in nonclinical studies. Toxicol Pathol. **50**: 512–530. 2022. [Medline] [CrossRef]
49. Bradley AE, Wancket LM, Rinke M, Gruebbel MM, Saladino BH, Schafer K, Katsuta O, Garcia B, Chanut F, Hughes K, Nelson K, Himmel L, McInnes E, Schucker A, and Uchida K. International Harmonization of Nomenclature and Diagnostic Criteria (INHAND): nonproliferative and proliferative lesions of the rabbit. J Toxicol Pathol. **34**(Suppl): 183S–292S. 2021. [Medline] [CrossRef]